doi:10.1246/cl.2012.639
Published on the web June 2, 2012

Porous $ZnFe_2O_4$ Nanospheres Grown on Graphene Nanosheets as a Superior Anode Material for Lithium Ion Batteries

Xianglan Chen,[1,2] Bin Cheng,[1,2] Huayun Xu,[1,2] Jian Yang,*[1,2] and Yitai Qian[1,2,3,4]
[1]*Key Laboratory of Colloid and Interface Chemistry, Ministry of Education, Shandong University, Jinan 250100, P. R. China*
[2]*School of Chemistry and Chemical Engineering, Shandong University, Jinan 250100, P. R. China*
[3]*Hefei National Laboratory for Physical Science at Microscale, University of Science and Technology of China, Hefei, Anhui 230026, P. R. China*
[4]*Department of Chemistry, University of Science and Technology of China, Hefei, Anhui 230026, P. R. China*

(Received March 7, 2012; CL-120200; E-mail: yangjian@sdu.edu.cn)

A facile solvothermal approach has been developed to grow porous $ZnFe_2O_4$ nanospheres on the surface of graphene nanosheets. The porous structure of $ZnFe_2O_4$ and the presence of graphene could significantly improve the electrochemical performance of the composite. The composite exhibits the reversible capacities of 970 mA h g^{-1} at 50 mA g^{-1} and 700 mA h g^{-1} at 600 mA g^{-1}, suggesting its promising potential as a superior anode material for lithium ion batteries.

Transition-metal oxides have been widely investigated as promising anode materials for high-power lithium-ion batteries (LIBs) due to their relatively high theoretical capacities (600–1000 mA h g^{-1}).[1–3] Recently, much attention has been paid to the cubic spinel structure of Fe-based binary oxides MFe_2O_4 (M = Ni, Co, Zn, and Cu).[4–6] $ZnFe_2O_4$ stands out from the others, because of its high theoretical capacity (1072 mA h g^{-1}, according to nine moles Li per mole of $ZnFe_2O_4$).[7] But it suffers from low electron conductivity and aggregation of the particles caused by charge/discharge cycles.[8] In order to address these issues, $ZnFe_2O_4$ has to be controlled on the order of nanometers and hybridized with carbon materials. Nanoscale structure can effectively shorten Li^+ insertion/extraction pathways[9] and carbon additives can significantly improve electron conductivity.[10] Graphene, a monolayer of carbon atoms, shows superior electrical conductivity, high surface area, and good mechanical flexibility.[11] The characteristics provide a highly conductive matrix and offer a high contact area between electrolyte and electrode, facilitating transportation of Li^+ and electrons into the electrode. Thus, incorporating the nanoparticles with the graphene matrix can be an ideal strategy to improve specific capacity and cycling stability. However, to the best of our knowledge, an anode built with $ZnFe_2O_4$ and graphene-based materials for LIBs has not been reported.

Herein, we report a facile solvothermal method followed with an annealing process to synthesize a $ZnFe_2O_4$/graphene nanocomposite ($ZnFe_2O_4$/GC). The porous $ZnFe_2O_4$ nanospheres have an average diameter of about 250 nm, uniformly dispersing on graphene nanosheets. The hierarchical structure of $ZnFe_2O_4$/GC exhibits high a reversible capacity and a good rate capacity in LIBs.

All reagents were analytical grade and used without further purification. In a typical procedure, 24 mg of graphene oxide nanosheets, which were prepared by a chemical exfoliation process,[12] was added to 50 mL of ethylene glycol and followed by sonication to form a uniform dispersion. Then 2 mmol of $FeCl_3 \cdot 6H_2O$, 1 mmol of $ZnCl_2$, and 10 mmol of urea were added to the above dispersion under vigorously stirring. The mixed solution was transferred to a Teflon-lined stainless steel autoclave (60 mL) and heated at 200 °C for 24 h. The product was collected by centrifugation, washed with distilled water and ethanol, and dried at 80 °C in air for 8 h. Finally the powders were annealed at 500 °C for 3 h in a tube furnace under Ar to obtain the $ZnFe_2O_4$/GC composite.

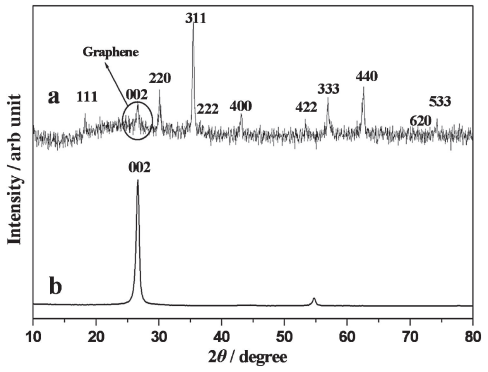

Figure 1. XRD patterns of $ZnFe_2O_4$/GC (a) and graphene (b).

Figure 1 shows the typical XRD patterns of the as-prepared $ZnFe_2O_4$/GC (a) and graphene (b). The diffraction peaks (Figure 1a) can be ascribed to cubic $ZnFe_2O_4$ with a space group of $Fd\bar{3}m$ (227) (JCPDS card No. 65-3111), except the peak at $2\theta = 26.5°$ that can be assigned to the (002) plane of graphene sheets (Figure 1b). The crystal size calculated by the Scherrer equation based on the XRD peaks, is 25.2 nm (Table S1, see Supporting Information, SI[17]).

Figures 2a and 2b show the SEM images of the product, in which the $ZnFe_2O_4$ nanospheres are uniformly attached to the surface of graphene nanosheets. The size and thickness of graphene nanosheets are 1–5 μm and 30–50 nm, respectively (Figure 2b and Figure S1, SI[17]). Some $ZnFe_2O_4$ nanospheres are inserted into the neighboring graphene nanosheets (Figure 2b), resulting in a sandwich-like architecture of the composite. The intimate contact between $ZnFe_2O_4$ nanospheres and graphene nanosheets generates a robust three-dimensional (3D) electron conduction network, increasing the electron conductivity. The separation of $ZnFe_2O_4$ nanospheres by graphene sheets also prevents their agglomeration during the charge/discharge processes. Figure 2c shows the particle sizes of the $ZnFe_2O_4$ nanospheres are in the range of 200–250 nm, consistent with the

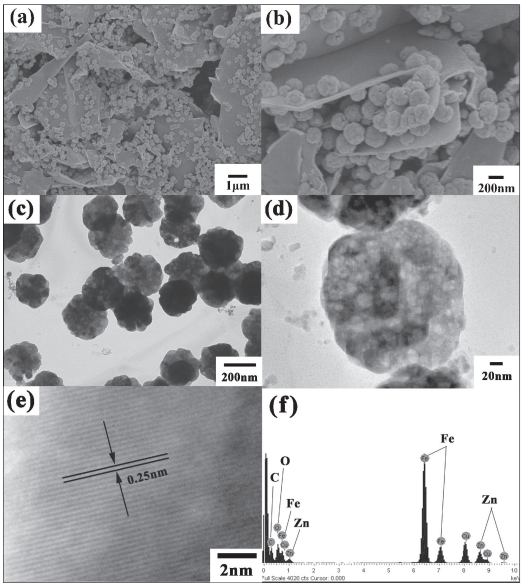

Figure 2. FESEM images (a, b), TEM image (c), HRTEM image (d, e), and EDS (f) of the $ZnFe_2O_4$/GC.

result of FESEM images. But this particle size is much larger than the crystal size obtained from the XRD peaks, indicating that nanospheres are composed of small crystals. Figure 2d presents a typical TEM image of a single nanosphere, in which the obvious contrast differences inside the single nanosphere indicate the presence of pores. The N_2 adsorption–desorption isotherm (Figure S2, SI[17]) further gives the pore size distribution around 21 nm, comparable with the crystal size of the product. The porous feature would promote the electrolyte penetration into the nanospheres, thus resulting in more interface areas between the electrode and the electrolyte. Figure 2e shows clear lattice fringes with a spacing of 0.25 nm, corresponding to the (311) planes of cubic $ZnFe_2O_4$. The energy-dispersive X-ray spectrum (EDS) (Figure 2f) of the composites shows the presence of C, Fe, O, and Zn. In addition, elementary analysis (EA) reveals the amount of graphene in $ZnFe_2O_4$/GC is approximately 10.1 wt %.

Figure 3 shows the charge–discharge profiles of the $ZnFe_2O_4$/GC electrode at a current density of 50 mA g^{-1} within a voltage range of 0.005–3.0 V vs. Li^+/Li. In the first discharge curve, the voltage continuously decreases to 0.9 V, which could be ascribed to the formation of $Li_xZnFe_2O_4$.[13–15] The voltage plateau at 0.9 V corresponds to a discharge capacity of ca. 200 mA h g^{-1}, in accordance with ca. 2 mol Li inserted into $ZnFe_2O_4$. The voltage then decreases to 0.8 V and produces a long and flat plateau. The lithium insertion capacity of this plateau is ca. 650 mA h g^{-1}, corresponding to a consumption of ca. 6 mol Li. This result might be caused by the reduction of Fe^{3+}, Fe^{2+}, and Zn^{2+} into metals.[13–15] Finally, the curve shows a gentle slope until 0.005 V, arising from the formation of the Li–Zn alloy.[13–15] The first charge profile shows a smoothly increasing plateau at 1.5–2.2 V due to the reverse reaction of the dealloying of Li–Zn alloy to Zn metal and the oxidation of Zn and Fe to Zn^{2+} and Fe^{2+}, Fe^{3+}. ZnO and Fe_2O_3 are believed to be the end products, because FeO could be further oxidized to Fe_2O_3 at high charge voltage.[13–15] The first discharge and charge

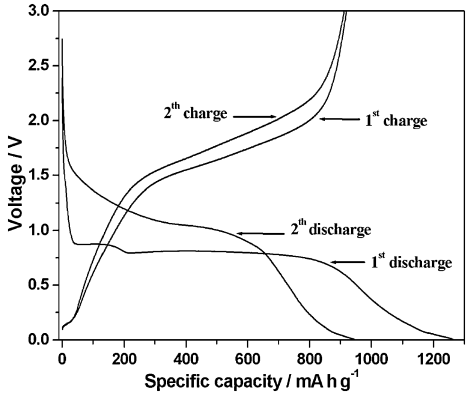

Figure 3. The initial two charge/discharge profiles of $ZnFe_2O_4$/GC between 0.005 and 3.0 V at a current density of 50 mA g^{-1}.

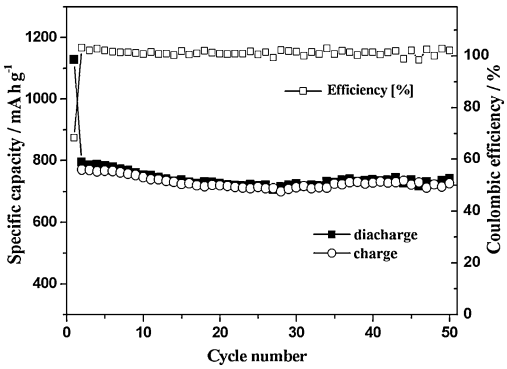

Figure 4. Cycling performance of the $ZnFe_2O_4$/GC electrode between 0.005 and 3.0 V at a current density of 300 mA g^{-1}.

capacities of $ZnFe_2O_4$/GC are as high as 1263 and 945 mA h g^{-1} at 50 mA g^{-1}. The initial Coulombic efficiency is only 74.8%, which might be attributed to the nature of the material and the formation of a solid electrolyte interphase (SEI) on the electrode surface due to the decomposition of the electrolyte.[14] In the second discharge curve, the voltage plateau shifts to around 1.0 V, while charge slope keeps steady at 1.5–2.2 V.

Figure 4 shows the cycle performance of the $ZnFe_2O_4$/GC between 0.005 and 3.0 V at 300 mA g^{-1}. The first discharge and charge capacities are 1128 and 770 mA h g^{-1}, corresponding to the Coulombic efficiency of 68.3%. The relatively low Coulombic efficiency could be ascribed to the incomplete oxidizing reactions, caused by the large particle size and the loss of electric contact.[14] It could be further improved by controlling the size, shape, and structure of the hybrid materials to shorten Li^+ diffusion pathway and increase electron conductivity. After the first cycle, the composite exhibits highly reversible behavior with the Coulombic efficiency about 100% and a reversible capacity about 741 mA h g^{-1} after 50 cycles. In order to illustrate the effect of graphene nanosheets, $ZnFe_2O_4$ prepared by the same solvothermal method without any graphene nanosheets is also tested as an anode material. At the current of 300 mA g^{-1}, the $ZnFe_2O_4$ nanoparticles show the first discharge and charge capacities about 1112.1 and 608 mA h g^{-1}, which decrease to 285.6 and 283.2 mA h g^{-1} after 50 cycles (Figure S3, SI[17]). This

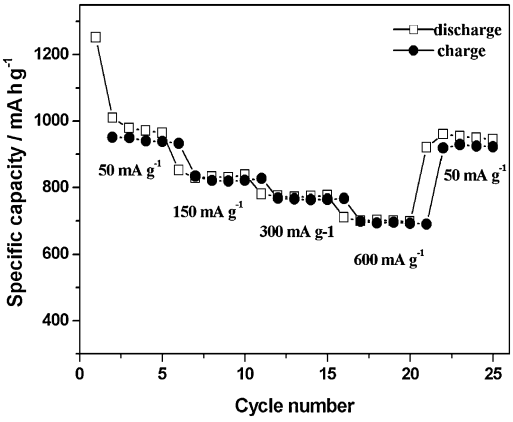

Figure 5. Rate capacity of the $ZnFe_2O_4$/GC electrode between 0.005 and 3.0 V at various current densities.

indicates that the $ZnFe_2O_4$/GC electrode has much higher capacities and better capacity retention than pure $ZnFe_2O_4$. The result might be related with the improved electron conductivity due to the presence of the graphene nanosheets, which has been confirmed by the electrochemical impedance spectra (Figure S4, SI[17]).

The $ZnFe_2O_4$/GC also displays a good rate capacity, as shown in Figure 5. The reversible capacity decreases from ca. 970 mA h g^{-1} at 50 mA g^{-1} to ca. 700 mA h g^{-1} at 600 mA g^{-1}, which is much higher than the theoretical capacity of a commercial graphite anode (372 mA h g^{-1}) and most of the previous reports about $ZnFe_2O_4$. Sharma and co-workers synthesized $ZnFe_2O_4$ nanoparticles in the size of 100–300 nm, and the nanoparticles only delivered a capacity about 615 mA h g^{-1} at a current density of 60 mA g^{-1} after 50 cycles.[13] $ZnFe_2O_4$ nanofibers obtained by electrospinning, kept a reversible specific capacity of 733 mA h g^{-1} at a current of 60 mA g^{-1} after 30 cycles.[16] Hollow $ZnFe_2O_4$ microspheres obtained by hydrothermal reactions exhibited a specific capacity of 500 mA h g^{-1} at 650 mA g^{-1}.[15] When the current density is back to 50 mA g^{-1}, the capacity returns to ca. 950 mA h g^{-1}, which almost recovers the initial capacity. The result indicates the good rate capability and stability of the composite as an anode.

The high reversible capacity, good cycling stability, and excellent rate capability of the $ZnFe_2O_4$/GC might be related with the hierarchical architecture composed of porous nanospheres and graphene nanosheets. First, the highly porous structure of $ZnFe_2O_4$ nanospheres facilitates the electrolyte transport and gives short diffusion paths of lithium ions as well. Second, the highly conducting 3D conductive network based on graphene promotes the fast electron transfer within electrode and current collector, thereby leading to a high specific capacity. Finally, graphene nanosheets also mitigate the crucial problem of agglomeration and provide more insertion/extraction lithium sites, resulting in large reversible capacity and cycling stability.

In summary, a facile solvothermal method has been developed to prepare $ZnFe_2O_4$/graphene composite by directly growing porous $ZnFe_2O_4$ nanospheres on graphene nanosheets. The composite has high first discharge and charge capacities of 1263 and 945 mA h g^{-1} at 50 mA g^{-1} and a good rate capability with a reversible capacity of 700 mA h g^{-1} at 600 mA g^{-1}. This $ZnFe_2O_4$/GC represents a promising candidate for anode material in LIBs, and the synthetic strategy can be easily extended to other electrode materials for better electrochemical performance.

We are also grateful for support of the 973 Project of China (No. 2011CB935901), the National Natural Science Found of China (No. 91022033 and No. 51172076), Independent Innovation Foundations of Shandong University (No. 2012ZD007) and start-up funding for new faculties in Shandong University.

References and Notes

1 X. Wang, X.-L. Wu, Y.-G. Guo, Y. Zhong, X. Cao, Y. Ma, J. Yao, *Adv. Funct. Mater.* **2010**, *20*, 1680.
2 N. Kijima, Y. Takahashi, H. Hayakawa, J. Awaka, J. Akimoto, *Chem. Lett.* **2007**, *36*, 568.
3 J. Wang, N. Du, H. Zhang, J. Yu, D. Yang, *J. Phys. Chem. C* **2011**, *115*, 11302.
4 R. Alcántara, M. Jaraba, P. Lavela, J. L. Tirado, J. C. Jumas, J. Olivier-Fourcade, *Electrochem. Commun.* **2003**, *5*, 16.
5 Y.-Q. Chu, Z.-W. Fu, Q.-Z. Qin, *Electrochim. Acta* **2004**, *49*, 4915.
6 M. Bomio, P. Lavela, J. L. Tirado, *J. Solid State Electrochem.* **2008**, *12*, 729.
7 Y. Ding, Y. Yang, H. Shao, *Electrochim. Acta* **2011**, *56*, 9433.
8 Y.-N. NuLi, Y.-Q. Chu, Q.-Z. Qin, *J. Electrochem. Soc.* **2004**, *151*, A1077.
9 Y. Wang, D. Su, A. Ung, J.-h. Ahn, G. Wang, *Nanotechnology* **2012**, *23*, 055402.
10 L. Jin, Y. Qin, H. Deng, W. Li, H. Li, S. Yang, *Electrochim. Acta* **2011**, *56*, 9127.
11 K. S. Novoselov, A. K. Geim, S. V. Morozov, D. Jiang, Y. Zhang, S. V. Dubonos, I. V. Grigorieva, A. A. Firsov, *Science* **2004**, *306*, 666.
12 X. Zhou, Z. Liu, *Chem. Commun.* **2010**, *46*, 2611.
13 Y. Sharma, N. Sharma, G. V. S. Rao, B. V. R. Chowdari, *Electrochim. Acta* **2008**, *53*, 2380.
14 Y. Deng, Q. Zhang, S. Tang, L. Zhang, S. Deng, Z. Shi, G. Chen, *Chem. Commun.* **2011**, *47*, 6828.
15 X. Guo, X. Lu, X. Fang, Y. Mao, Z. Wang, L. Chen, X. Xu, H. Yang, Y. Liu, *Electrochem. Commun.* **2010**, *12*, 847.
16 P. F. Teh, Y. Sharma, S. S. Pramana, M. Srinivasan, *J. Mater. Chem.* **2011**, *21*, 14999.
17 Supporting Information is available electronically on the CSJ-Journal Web site, http://www.csj.jp/journals/chem-lett/index.html.

